Affine Lines in Spheres

Andrew Stimpson

October 20, 2003

1 Introduction

Because of the hairy ball theorem, the only closed 2-manifold that supports a lattice in its tangent space is T^2. But, if singular points (i.e. points whose tangent space is not endowed with 2 distinct coordinate directions) are allowed, then it becomes possible to give the tangent space a lattice. Because the lattice is well defined everywhere around the points, the effect of moving around the singular points must map the lattice in the tangent space to itself, and as such, the holonomy of the points must be in $\mathrm{SL}(2,\mathbb{Z})$. This endows the manifold (minus the singular points) with an integral affine structure. This gives every point a sense of direction, but is not quite a metric (for that the holonomy of every point would also have to be in $\mathrm{SO}(2,\mathbb{R})$, giving each singularity a finite amount of Gaussian curvature). Thus, one can have paths in the manifold that are "straight lines" in some sense, which we refer to *affine lines*.

The choices of the types of singular points yields varying affine structures. This paper investigates visualizing one particular type of construction of the the singular points for S^n given in the first two sections of "Integral Affine Structures on Spheres I" by Christian Haase and Ilia Zharkov [1] for the case where $n = 2$, as well as the affine lines in a particular example. This yields insight to the more general case.

Acknowledgements. This work was completed while participating in the Research Experience for Undergraduates (made possible by a a grant from VIGRE), working with Dr. Margaret Symington of the School of Mathematics at the Georgia Institute of Technology during the summer of 2003.

2 Input

2.1 Reflexive polytopes

A convex polytope is defined as either the convex hull of a finite set of points $X = \{x^1, \ldots, x^n\}$ in $\mathbb{R}^d$:

$$\mathrm{conv}\,(X) \equiv \left\{ \sum_{i=1}^{n} \lambda_i x^i \,\middle|\, \lambda_i \geq 0, \sum_{i=1}^{n} \lambda_i = 1 \right\}. \tag{1}$$

or the bounded solution set of a finite system of linear inequalities:

$$P(A,b) \equiv \left\{ x \in \mathbb{R}^d \middle|\, a_i^T\, x \leq b_i \text{ for } 1 \leq i \leq m \right\} \tag{2}$$

where $A \in \mathbb{R}^{m\times d}$ is a real matrix with rows a_i^T and $b \in \mathbb{R}^m$. Both constructions are equivalent, i.e. for every pair of a matrix A and vector b, there exists a finite set of points X such that $\mathrm{conv}\,(X) = P(A,b)$, and vice versa. One can obtain the *dual polytope* by exchanging the roles of x^i and a_i^T. [2] Geometrically, the corresponds to exchanging facets with vertices, or in other words, the homology on a polytope is the cohomology on its dual and vice versa.

The combinatorial model given in [1] requires the choice of an *reflexive polytope*. A reflexive polytope has all its vertices and dual vertices in $\mathbb{Z}^d$ (with $b_i = 1$). Note that a reflexive polytope must contain the origin (or else its dual becomes unbounded, and not the convex hull of a set of finite set of points). A necessary (but not sufficient) condition for a polytope to be reflexive is for the components of each vertex to be relatively prime. To see this, suppose we have a a vertex (kp, kq, kr) where p, q, and r are all relatively prime. The facet in the dual polytope determined by vertex will be in the plane

$$\left\{ v \in \mathbb{R}^3 \middle|\, \langle v, (kp, kq, kr)\rangle = 1 \right\} \tag{3}$$

But if $v \in \mathbb{Z}^3$, then then $\langle v, (kp, kq, kr)\rangle$ will be a multiple of k. Therefore, if $k \neq 1$, then the plane described in Eqn. (3) will not have any point in $\mathbb{Z}^3$. Since all vertices in this facet are in this plane, none of them can be in $\mathbb{Z}^3$, and and thus this cannot be a reflexive polytope.

The polytope (and its dual) used in our discussion (and the primary example in [1]) are shown in Fig. 1. The polytope is

$$\Delta^\vee = \mathrm{conv}\left(\begin{bmatrix} 0 \\ 0 \\ -1 \end{bmatrix}, \begin{bmatrix} 1 \\ 1 \\ 1 \end{bmatrix}, \begin{bmatrix} 1 \\ -1 \\ 1 \end{bmatrix}, \begin{bmatrix} -1 \\ 1 \\ 1 \end{bmatrix}, \begin{bmatrix} -1 \\ -1 \\ 1 \end{bmatrix} \right) \tag{4}$$

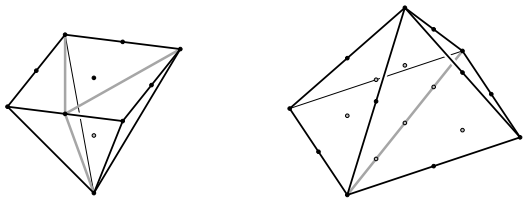

(a) $\Delta^\vee$ (b) Δ

Figure 1: The reflexive polytope examined.

and its dual polytope is

$$\Delta = \text{conv}\left(\begin{bmatrix}0\\0\\1\end{bmatrix}, \begin{bmatrix}2\\0\\-1\end{bmatrix}, \begin{bmatrix}-2\\0\\-1\end{bmatrix}, \begin{bmatrix}0\\2\\-1\end{bmatrix}, \begin{bmatrix}0\\-2\\-1\end{bmatrix}\right). \tag{5}$$

2.2 Coherent triangulations

The gray lines in Fig. 1 along with the actual edges of the polytope represent a *coherent triangulation* of the polytopes. This triangulation is generated by imagining the polytope as sitting in the subspace of $\mathbb{R}^4$ that has the fourth component zero. Then each point of $\mathbb{Z}^3 \cap \Delta^\vee$ is given an integer "height" in this extra direction. This collection of heights is the "sufficiently generic vector", ν, described in [1]. We take the convex hull of this new collection of vertices in $\mathbb{Z}^4$. This generates a new collection of facets and edges. Then we project the fourth component we added back out again, but remembering where the new edges were created when we "folded" it up into the extra dimension. This creates a triangulation of the surface of the solid polytope that restricts to a triangulation of the surface as well (which is in essence, what a coherent triangulation is). This entire process is also repeated with the dual polytope, Δ and its sufficiently generic vector, λ.

This means that the condition of being "sufficiently generic" is defined as making sure enough "folds" occur such that each of the new (internal and external) facets created in the polytope is a simplex. In the example in Fig. 1, all the gray edges connect vertices that had their auxiliary heights set to equal values.

3 The Combinatorial construction

3.1 The induced "triangulation" of S^2

Using the definition of a polytope given in Eqn. (2), we can see that

$$\Delta^\vee = \left\{n \in \mathbb{R}^3 : \langle n, m\rangle \leq 1 \, \forall m \in \Delta\right\} \tag{6}$$
$$\Delta = \left\{m \in \mathbb{R}^3 : \langle m, n\rangle \leq 1 \, \forall n \in \Delta^\vee\right\}. \tag{7}$$

Thus we consider a complex Σ in $\mathbb{R}^6$ which has a base space

$$|\Sigma| = \left\{(m, n) \in \Delta \times \Delta^\vee : \langle m, n\rangle = 1\right\}. \tag{8}$$

Note that this will actually be a subset of $\partial\Delta \times \partial\Delta^\vee$ since it is only at the boundary that the extremal values of the inequalities in Eqs. (6) and (7) be reached. It is proved in [1] that this base space in fact a sphere. One expects the space to indeed be a 2-dimensional manifold since every vertex, edge, or facet of $\Delta^\vee$ corresponds to a facet, edge, or vertex of Δ respectively. Therefore the cartesian product of any of these pairs of objects will have dimension two.

Any triangulations of $\Delta^\vee$ and Δ induce a "triangulation" of $\Delta \times \Delta^\vee$ in the natural way: elements of this combinatorial object are the cartesian product of simplices in $\Delta^\vee$ with simplices in Δ. Let S and T be the coherent triangulations of Δ and $\Delta^\vee$ respectively as described above. Define Σ as the restriction of $\mathrm{bsd}\,(S) \times \mathrm{bsd}\,(T)$ to $|\Sigma|$, where $\mathrm{bsd}\,(\cdot)$ denotes the barycentric subdivision.

3.2 Atlas construction and singular points

This construction of Σ gives two natural simplicial projection maps,

$$p_1 : \Sigma \to \mathrm{bsd}\,(S) \qquad \text{and} \qquad p_2 : \Sigma \to \mathrm{bsd}\,(T), \tag{9}$$

each of which project the second and first component respectively. Then for each vertex $v \in S$ and each vertex $w \in T$, we define

$$U_v \equiv p_1^{-1}(\mathrm{star}_{\mathrm{bsd}(S)}(v)) \qquad \text{and} \qquad V_w \equiv p_2^{-1}(\mathrm{star}_{\mathrm{bsd}(T)}(w)) \tag{10}$$

where these are the preimages of open stars in their respective subdivisions. Note that any U_v or V_w will always contain the facet that is dual to v or w respectively. Since each these sets will be homeomorphic to an open disk, this provides an atlas for $\Sigma - D$, where D is the singular locus, which is defined as the full subcomplex that

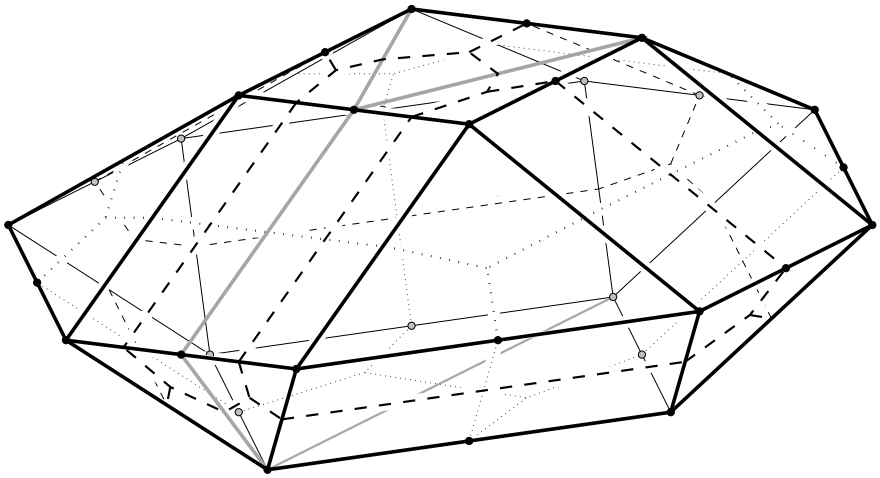

Figure 2: The induced "triangulation" of S^2, $|\Sigma|$.

is induced by $(\hat{\sigma}, \hat{\tau})$ where neither $\sigma \in S$ and $\tau \in T$ are 0-dimensional simplices. We define $\hat{\sigma} \in \mathrm{bsd}\,(S)$ as the simplex that is the barycenter of σ (and likewise for τ).

In our particular example, the only possible values of (σ, τ) are when σ is an edge of a facet in Δ and τ is an edge of facet in $\Delta^\vee$. This can be seen in the Fig. 2: dotted lines indicate the boundaries of the U_v's, and dashed for the V_w's. Thus the singular locus consists of a 9 points, which are the intersection of the dashed and dotted lines.

To truly be an atlas, we must specify the transition maps that define how do move from one coordinate patch to another on the overlapping points. How actual points get mapped is obvious[1], but since we want to embed a lattice in the tangent space of this sphere, we must also specify how to move between the tangent spaces of each coordinate map as well. To do this, we identify the tangent space at each point $q \in \Sigma$ with $\boldsymbol{T}_q$ and the corresponding lattice $\boldsymbol{T}_q^{\mathbb{Z}}$. If $q \in U_v$ for some vertex $v \in S$, then they are defined as

$$\boldsymbol{T}_q = \mathbb{R}_v^3 \equiv \left\{ n \in \mathbb{R}^3 : \langle v, n \rangle = 0 \right\} \qquad \text{and} \qquad \boldsymbol{T}_q^{\mathbb{Z}} = \mathbb{Z}_v^3 \equiv \mathbb{R}_v^3 \cap \mathbb{Z}^3. \tag{11}$$

[1]This is because the tangent space transition maps determine the coordinate transition maps up to a constant, but there is only one choice of constant that will work with the open cover of $\Sigma - D$. Any choice other than the natural one won't work since the coordinate patches won't line up anymore.

If $q \in V_w$ for some vertex $w \in T$, then they are defined as the quotients

$$\boldsymbol{T}_q = \mathbb{R}^3/w \qquad \text{and} \qquad \boldsymbol{T}_q = \mathbb{Z}^3/w. \tag{12}$$

These two definitions seem quite similar—indeed, as just tangent spaces, they must be isomorphic. The difference lies in the lattices, which are quite different. If we were to identify the first quotient in Eq. (12) with the 2-dimensional subspace of $\mathbb{R}^3$ that is orthogonal to w (as in Eq. (11)), to keep the same lattice, we would have to orthogonally project all of $\mathbb{Z}^3$ onto this subspace (whereas the lattice in Eq. (11) is the *intersection* of $\mathbb{Z}^3$ with the subspace). Note that this projection can't be dense on the subspace since $w \in \mathbb{Z}^3$. So in both cases, there is a choice of basis for each coordinate patch such that the lattice is parameterized by $\mathbb{Z}^2$.

4 Lines

4.1 Transition maps

With this machinery, we can define the transition map $f_{vw} : \mathbb{R}^3_v \to \mathbb{R}^3/w$ with the natural projection map of $\mathbb{R}^3 \to \mathbb{R}^3/w$ restricted to the subspace $\mathbb{R}^3_v$. Since we are guaranteed that $\langle v, w\rangle = 1 \; \forall \, v, w$, this map will always be invertible. Also, it maps both versions of $\boldsymbol{T}^{\mathbb{Z}}_q$ onto each other (Lemma 2.4 of [1] provides an elementary proof).

For calculation purposes, we choose a the subspace orthogonal to w as a fundamental domain for $\mathbb{R}^3/d$. This makes the natural quotient projection literally an orthogonal projection. So you can visualize the effect of moving a tangent vector on a facet in Σ that is the product of a vertex in Δ and a facet in $\Delta^\vee$ (which will live in some U_v) to a facet in Σ that is the product of a facet in Δ and a vertex in $\Delta^\vee$ (which will live in some V_w) by sliding the vector of the first facet in Σ off the edge of the facet and into the space above the second facet in Σ, and then just dropping it down onto that second facet.

As an example, let $v = (0, 0, 1)$ and $w = (1, 1, 1)$. Then U_v is the coordinate patch that contains the facet on the top of of the polytope in Fig. 2, and V_w is the coordinate patch that covers the triangle facet facing towards the page. Choosing $\{(1, 0, 0), (0, 1, 0)\}$ as a basis for $\mathbb{R}^3_v$, and $\{(1, 1, -2), (1, -1, 0)\}$ as a basis for our fundamental domain of $\mathbb{R}^3/w$, we get that the transition map $f_{(1,0,0)(1,1,1)}$ for the tangent space is

$$f_{(1,0,0)(1,1,1)}(x, y) = M \begin{pmatrix} x \\ y \end{pmatrix} \tag{13}$$

(a) U_v's

v	Basis vectors
$(0,0,1)$	$(1,0,0),(0,1,0)$
$(2,0,-1)$	$(1,0,2),(0,1,0)$
$(0,2,-1)$	$(1,0,0),(0,1,2)$
$(-2,0,-1)$	$(1,0,-2),(0,1,0)$
$(0,-2,-1)$	$(1,0,0),(0,1,-2)$

(b) V_w's

w	Basis vectors
$(0,0,-1)$	$(1,0,0),(0,1,0)$
$(1,-1,1)$	$(1,1,0),(1,-1,-2)$
$(1,1,1)$	$(1,1,-2),(1,-1,0)$
$(-1,1,1)$	$(1,1,0),(1,-1,2)$
$(-1,-1,1)$	$(1,1,2),(1,-1,0)$
$(1,0,1)$	$(1,0,-1),(0,1,0)$

Table 1: The choice of basis vectors for each coordinate patch in our primary example.

where

$$M = \begin{pmatrix} 1 & 1 & -2 \\ 1 & -1 & 0 \end{pmatrix} \begin{pmatrix} 1 & 0 \\ 0 & 1 \\ 0 & 0 \end{pmatrix} = \begin{pmatrix} 1 & 1 \\ 1 & -1 \end{pmatrix}. \tag{14}$$

Table 1 gives a choice of basis vectors for each coordinate patch, and and Table 2 gives the transition matrices for all the overlapping coordinate patches, which were calculated analogously to Eq. (14).

4.2 Monodromy

By multiplying the matrices from Table 2 together, we can calculate what the total effect of moving a tangent vector around one of the singular points, or the monodromy of the path taken. For example, if one starts on $V_{(1,1,1)}$, the combined monodromy of the pair of singular points that are on the same facet in Σ is

$$\begin{aligned} &M_{(1,1,1)\leftarrow(2,0,-1)} M_{(2,0,-1)\leftarrow(1,-1,1)} M_{(1,-1,1)\leftarrow(0,0,1)} M_{(0,0,1)\leftarrow(1,1,1)} \\ &\quad = \begin{pmatrix} -3 & 1 \\ 1 & -1 \end{pmatrix} \frac{1}{2} \begin{pmatrix} -1 & -1 \\ 3 & 1 \end{pmatrix} \begin{pmatrix} 1 & 1 \\ 1 & -1 \end{pmatrix} \frac{1}{2} \begin{pmatrix} 1 & 1 \\ 1 & -1 \end{pmatrix} = \begin{pmatrix} 3 & 2 \\ -2 & -1 \end{pmatrix} \end{aligned} \tag{15}$$

As mentioned before, these transition maps send $\boldsymbol{T}_q^{\mathbb{Z}}$ to itself; so in our choice of basis, the monodromy of any path will map $\mathbb{Z}^2$ to itself and thus be in $\mathrm{SL}(2,\mathbb{Z})$.

<insert stuff about the how the monodromies always have an eigendirection>

The first step in identifying loops that are potential straight lines is identifying the homotopy classes of loops that have trivial monodromy. In a neighborhood around such a loop, we can construct a flat metric. We expect such a metric to

v	w	$U_v \to V_w$	$V_w \to U_v$
$(0,0,1)$	$(1,-1,1)$	$\begin{pmatrix} 1 & 1 \\ 1 & -1 \end{pmatrix}$	$\frac{1}{2}\begin{pmatrix} 1 & 1 \\ 1 & -1 \end{pmatrix}$
$(0,0,1)$	$(1,1,1)$	$\begin{pmatrix} 1 & 1 \\ 1 & -1 \end{pmatrix}$	$\frac{1}{2}\begin{pmatrix} 1 & 1 \\ 1 & -1 \end{pmatrix}$
$(0,0,1)$	$(-1,1,1)$	$\begin{pmatrix} 1 & 1 \\ 1 & -1 \end{pmatrix}$	$\frac{1}{2}\begin{pmatrix} 1 & 1 \\ 1 & -1 \end{pmatrix}$
$(0,0,1)$	$(-1,-1,1)$	$\begin{pmatrix} 1 & 1 \\ 1 & -1 \end{pmatrix}$	$\frac{1}{2}\begin{pmatrix} 1 & 1 \\ 1 & -1 \end{pmatrix}$
$(0,0,1)$	$(1,0,1)$	$\begin{pmatrix} 1 & 0 \\ 0 & 1 \end{pmatrix}$	$\begin{pmatrix} 1 & 0 \\ 0 & 1 \end{pmatrix}$
$(2,0,-1)$	$(0,0,-1)$	$\begin{pmatrix} 1 & 0 \\ 0 & 1 \end{pmatrix}$	$\begin{pmatrix} 1 & 0 \\ 0 & 1 \end{pmatrix}$
$(2,0,-1)$	$(1,-1,1)$	$\begin{pmatrix} 1 & 1 \\ -3 & -1 \end{pmatrix}$	$\frac{1}{2}\begin{pmatrix} -1 & -1 \\ 3 & 1 \end{pmatrix}$
$(2,0,-1)$	$(1,1,1)$	$\begin{pmatrix} -3 & 1 \\ 1 & -1 \end{pmatrix}$	$-\frac{1}{2}\begin{pmatrix} 1 & 1 \\ 1 & 3 \end{pmatrix}$
$(2,0,-1)$	$(1,0,1)$	$\begin{pmatrix} -1 & 0 \\ 0 & 1 \end{pmatrix}$	$\begin{pmatrix} -1 & 0 \\ 0 & 1 \end{pmatrix}$
$(0,2,-1)$	$(0,0,-1)$	$\begin{pmatrix} 1 & 0 \\ 0 & 1 \end{pmatrix}$	$\begin{pmatrix} 1 & 0 \\ 0 & 1 \end{pmatrix}$
$(0,2,-1)$	$(1,1,1)$	$\begin{pmatrix} 1 & -3 \\ 1 & -1 \end{pmatrix}$	$\frac{1}{2}\begin{pmatrix} -1 & 3 \\ -1 & 1 \end{pmatrix}$
$(0,2,-1)$	$(-1,1,1)$	$\begin{pmatrix} 1 & 1 \\ 1 & 3 \end{pmatrix}$	$\frac{1}{2}\begin{pmatrix} 3 & -1 \\ -1 & 1 \end{pmatrix}$
$(-2,0,-1)$	$(0,0,-1)$	$\begin{pmatrix} 1 & 0 \\ 0 & 1 \end{pmatrix}$	$\begin{pmatrix} 1 & 0 \\ 0 & 1 \end{pmatrix}$
$(-2,0,-1)$	$(-1,1,1)$	$\begin{pmatrix} 1 & 1 \\ -3 & -1 \end{pmatrix}$	$\frac{1}{2}\begin{pmatrix} -1 & -1 \\ 3 & 1 \end{pmatrix}$
$(-2,0,-1)$	$(-1,-1,1)$	$\begin{pmatrix} -3 & 1 \\ 1 & -1 \end{pmatrix}$	$-\frac{1}{2}\begin{pmatrix} 1 & 1 \\ 1 & 3 \end{pmatrix}$
$(0,-2,-1)$	$(0,0,-1)$	$\begin{pmatrix} 1 & 0 \\ 0 & 1 \end{pmatrix}$	$\begin{pmatrix} 1 & 0 \\ 0 & 1 \end{pmatrix}$
$(0,-2,-1)$	$(-1,-1,1)$	$\begin{pmatrix} 1 & -3 \\ 1 & -1 \end{pmatrix}$	$\frac{1}{2}\begin{pmatrix} -1 & 3 \\ -1 & 1 \end{pmatrix}$
$(0,-2,-1)$	$(1,-1,1)$	$\begin{pmatrix} 1 & 1 \\ 1 & 3 \end{pmatrix}$	$\frac{1}{2}\begin{pmatrix} 3 & -1 \\ -1 & 1 \end{pmatrix}$

Table 2: The matrices that define the transition maps for our primary example.

exist because the only things impeding us from expanding a coordinate patch over the entire sphere are the singular points. So the loops with trivial monodromy actually represent "ribbons" in the sphere that are Ricci flat. This can only be extended to other regions if the monodromy of a set singular points is in SO(2,$\mathbb{R}$), in which case that set of singularities possess a finite amount of Gaussian curvature. The only candidate monodromies are rotations by integer multiples of $\pi/2$, which are the only elements in $\mathrm{SO}(2,\mathbb{R})$ and $\mathrm{SL}(2,\mathbb{Z})$.

4.3 Families of lines found

Because we are also searching for lines that break the sphere into two parts, any potential candidates cannot cross themselves. This constraint gives us only finitely many candidate loops, and thus by exhaustively calculating the monodromies of all of them, we can separate them into four distinct classes, which are shown in Fig. 3. The construction of the figure was motivated as follows:

Previously, we described the action of the projection that defines the transition maps as an orthogonal projection of vectors in the U_v's to vectors in the V_w's. In Fig. 3, all the points covered by a V_w were projected into the corresponding $\mathbb{R}^3/w$. The the separate coordinate patches were glued together where possible. Thus, inside the dashed lines, affine straight lines correspond to actual Ricci straight lines. However, whenever a liner crosses into another V_w, the lines get bent (i.e., the tangent vector gets multiplied by the appropriate transition matrix).

Because of the way the orthogonal projection works, this makes the eigendirection for each singularity point in a direction perpendicular to the dashed lines (if an analogous diagram were constructed using the U_v's instead, the eigendirection would be parallel to the coordinate patch boundaries). This means that the four families of lines in Fig. 3 are actually only two families: the pairs that run parallel to each other can be slid right through the singular points on the boundaries of the square in the center.

5 Nonsymmetric Example

A natural question to ask is whether any such choice of a reflexive polytope and its dual along with a coherent triangulation for each leads to such an integral affine structure for S^2 that admits these straight lines. One might be tempted to believe that the requirements on the polytopes and triangulation enforces some minimal level of symmetry that would always yield the straight lines. However, consider

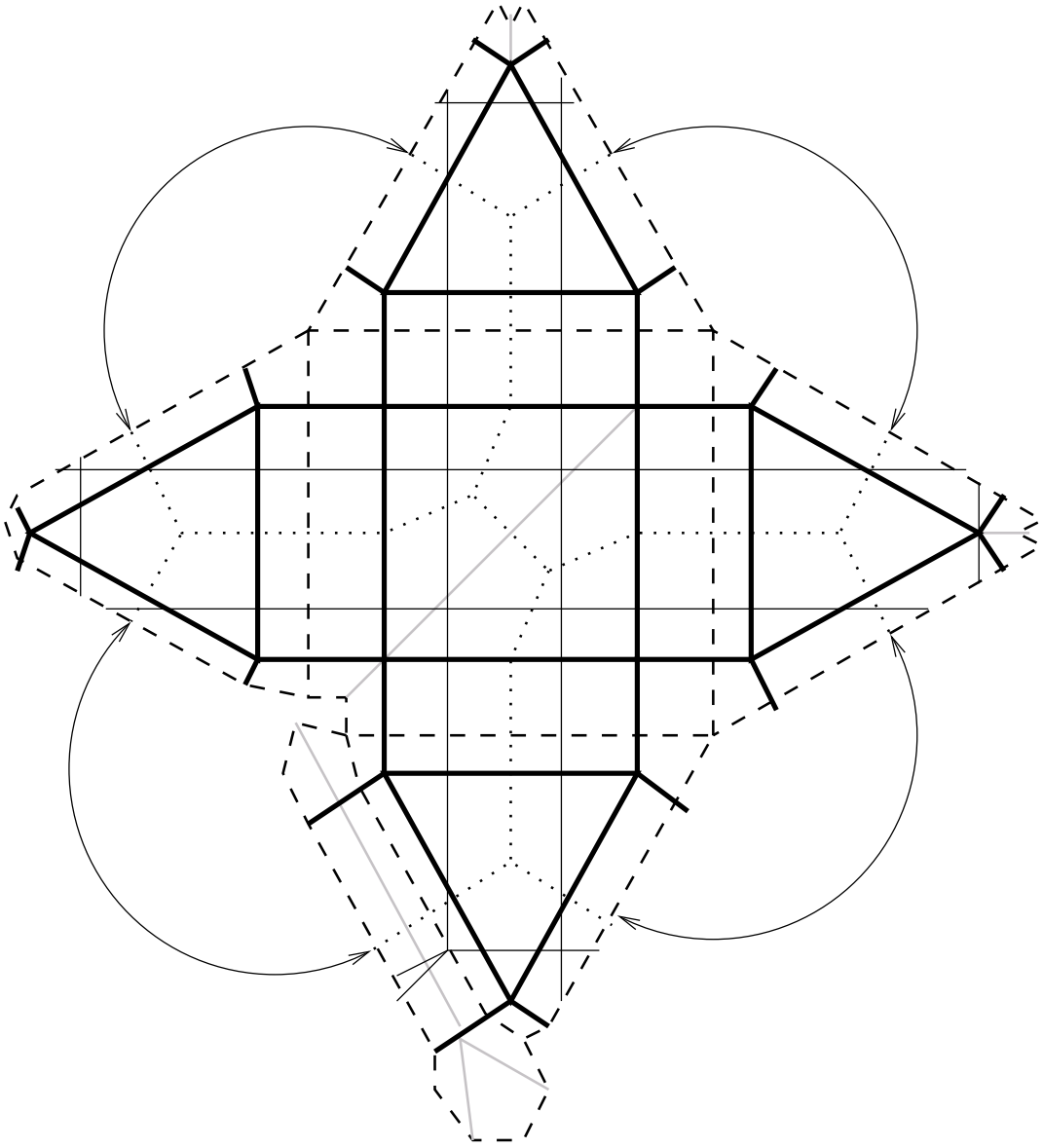

Figure 3: The primary example, unfolded. All the different types of lines in Fig. 2 are preserved. The thin solid back lines represent the four families of affine straight lines, and the circular arcs show which singular points get identified when the polytope is "folded back up."

the following tetrahedron $\Gamma^\vee$

$$\Gamma^\vee = \text{conv}\left(\begin{bmatrix}0\\-2\\1\end{bmatrix}, \begin{bmatrix}-4\\2\\1\end{bmatrix}, \begin{bmatrix}4\\2\\1\end{bmatrix}, \begin{bmatrix}0\\0\\1\end{bmatrix}\right) \tag{16}$$

and its dual tetrahedron Γ

$$\Gamma = \text{conv}\left(\begin{bmatrix}0\\1\\-1\end{bmatrix}, \begin{bmatrix}1\\-1\\-1\end{bmatrix}, \begin{bmatrix}-1\\-1\\-1\end{bmatrix}, \begin{bmatrix}0\\0\\1\end{bmatrix}\right). \tag{17}$$

Since a tetrahedron is already a 3-simplex, give both polytopes the trivial triangulation. There are only a finite number of elements in the fundamental group of the $\Sigma - D$ generated by this input that could possibly break the sphere into two parts (again, there is the no self-intersection criterion). By exhaustive search, we have determined that there are *no* such loops that have trivial monodromy. The polytopes' complete lack of isometric symmetries seems to be the culprit in this case.

6 Comments and Observations

While the choice of polytopes has an obvious effect on the induced affine structure, the consequences of the choice of coherent triangulations is more subtle. In the primary example, having a "combinatorial" vertex in the middle of an edge causes the what would otherwise be one singularity to split into two. The monodromy around both of them is the same as it would be for one singularity; the only difference is that there is a new coordinate patch that corresponds to the added generator in the fundamental group of $\Sigma - D$.

One would hope that perhaps any possible choice of embedding these singularities in the tangent space of a sphere would yield something that is homeomorphic to one of these combinatorial constructions. The advantage of this would be that there are only finitely many such constructions: there are only finitely many reflexive polytopes, and according to [1] there can be at most 24 singular points in this 2-dimensional construction, which means that the coherent triangulations can't make things *too* difficult. Thus, this approach could lead to a classification theorem of all possible integral affine structures on S^2.

The obvious advantage to being able to identify straight lines would be that it would cut the classification problem in half: every polytope construction could be

broken down into two separate parts that are joins by a flat ribbon. Since our last examples fails to exhibit this behavior, it might be necessary to relax the condition of straight lines having trivial monodromy. All we require is that the tangent vector along the path be an eigenvector of the monodromy. This also might mean that there might not be a *family* of straight lines, only a finite number of them.

References

[1] Christian Haase and Ilia Zharkov. Integral affine structures on spheres and torus fibrations of calabi-yau toric hypersurfaces I. Technical Report DUKE-CGTP-02-05, Duke University, May 2002, math.AG/0205321.

[2] Martin Henk, Jürgen Richter-Gerbert, and Günter M. Ziegler. Basic properties of convex polytopes. In Jacob E. Goodman and Joseph O'Rourke, editors, *Handbook of Discrete and Computational Geometry*, chapter 13, pages 243–269. CRC-Press, New York, 1997.